AD_____

CONTRACT NO: DAMD17-95-C-5038

TITLE: Perimetric Mapping of Hyperacuity: Effects of Retinal Laser Scars

PRINCIPAL INVESTIGATOR(S): Elmar T. Schmeisser, Ph.D.

CONTRACTING ORGANIZATION: University of Kentucky Research Foundation
Lexington, Kentucky 40506-0056

REPORT DATE: June 1996

TYPE OF REPORT: Midterm

PREPARED FOR: U.S. Army Medical Research and Materiel Command
Fort Detrick, Frederick, Maryland 21702-5012

REPORT DOCUMENTATION PAGE

Form Approved
OMB No. 0704-0188

1. AGENCY USE ONLY (Leave blank)	2. REPORT DATE	3. REPORT TYPE AND DATES COVERED
	June 1996	Midterm (25 May 95 - 24 May 96)

4. TITLE AND SUBTITLE

Perimetric Mapping of Hyperacuity: Effects of Retinal Laser Scars

5. FUNDING NUMBERS

DAMD17-95-C-5038

6. AUTHOR(S)

Elmar T. Schmeisser, Ph.D.

7. PERFORMING ORGANIZATION NAME(S) AND ADDRESS(ES)

University of Kentucky Research Foundation
Lexington, Kentucky 40506-0056

8. PERFORMING ORGANIZATION REPORT NUMBER

9. SPONSORING/MONITORING AGENCY NAME(S) AND ADDRESS(ES)

U.S. Army Medical Research and Materiel Command
Fort Detrick
Frederick, Maryland 21702-5012

10. SPONSORING/MONITORING AGENCY REPORT NUMBER

11. SUPPLEMENTARY NOTES

12a. DISTRIBUTION/AVAILABILITY STATEMENT

Approved for public release; distribution unlimited

13. ABSTRACT *(Maximum 200 words)*

The effects of specific graded retinal laser lesions on both hyperacuity and local luminance perimetry were measured by electrophysiological means. Animals were used that previously received minimal spot laser exposures from a pulsed neodymium-YAG laser at energies up to and including contained subretinal hemorrhages in both the parafovea and the fovea. In these experiments, a 95% contrast vernier acuity targets were presented at high luminance levels to anesthetized primates. Visual evoked potentials were recorded by conventional means. An additional map of each retina was produced by flickering small patches on the stimulus display and recording the retinal signal. Vernier recording have proven relatively successful in those animals with less than contained retinal hemmorage lesions in the fovea. Animals with such lesions have grossly degraded resolution acuity and no recordable vernier acuity. Retinal and cortical topographic function mapping has to date proven unsuccessful.

14. SUBJECT TERMS	15. NUMBER OF PAGES
Acuity, Aiming, ERG, Eye, Laser, Lesion, Primate, Retina, VEP	41
	16. PRICE CODE

17. SECURITY CLASSIFICATION OF REPORT	18. SECURITY CLASSIFICATION OF THIS PAGE	19. SECURITY CLASSIFICATION OF ABSTRACT	20. LIMITATION OF ABSTRACT
Unclassified	Unclassified	Unclassified	Unlimited

GENERAL INSTRUCTIONS FOR COMPLETING SF 298

The Report Documentation Page (RDP) is used in announcing and cataloging reports. It is important that this information be consistent with the rest of the report, particularly the cover and title page. Instructions for filling in each block of the form follow. It is important to *stay within the lines* to meet ***optical scanning requirements***.

Block 1. Agency Use Only *(Leave blank)*.

Block 2. Report Date. Full publication date including day, month, and year, if available (e.g. 1 Jan 88). Must cite at least the year.

Block 3. Type of Report and Dates Covered. State whether report is interim, final, etc. If applicable, enter inclusive report dates (e.g. 10 Jun 87 - 30 Jun 88).

Block 4. Title and Subtitle. A title is taken from the part of the report that provides the most meaningful and complete information. When a report is prepared in more than one volume, repeat the primary title, add volume number, and include subtitle for the specific volume. On classified documents enter the title classification in parentheses.

Block 5. Funding Numbers. To include contract and grant numbers; may include program element number(s), project number(s), task number(s), and work unit number(s). Use the following labels:

C	- Contract	**PR**	- Project
G	- Grant	**TA**	- Task
PE	- Program Element	**WU**	- Work Unit Accession No.

Block 6. Author(s). Name(s) of person(s) responsible for writing the report, performing the research, or credited with the content of the report. If editor or compiler, this should follow the name(s).

Block 7. Performing Organization Name(s) and Address(es). Self-explanatory.

Block 8. Performing Organization Report Number. Enter the unique alphanumeric report number(s) assigned by the organization performing the report.

Block 9. Sponsoring/Monitoring Agency Name(s) and Address(es). Self-explanatory.

Block 10. Sponsoring/Monitoring Agency Report Number. *(If known)*

Block 11. Supplementary Notes. Enter information not included elsewhere such as: Prepared in cooperation with...; Trans. of...; To be published in.... When a report is revised, include a statement whether the new report supersedes or supplements the older report.

Block 12a. Distribution/Availability Statement. Denotes public availability or limitations. Cite any availability to the public. Enter additional limitations or special markings in all capitals (e.g. NOFORN, REL, ITAR).

- DOD - See DoDD 5230.24, "Distribution Statements on Technical Documents."
- DOE - See authorities.
- NASA - See Handbook NHB 2200.2.
- NTIS - Leave blank.

Block 12b. Distribution Code.

- DOD - Leave blank.
- DOE - Enter DOE distribution categories from the Standard Distribution for Unclassified Scientific and Technical Reports.
- NASA - Leave blank.
- NTIS - Leave blank.

Block 13. Abstract. Include a brief *(Maximum 200 words)* factual summary of the most significant information contained in the report.

Block 14. Subject Terms. Keywords or phrases identifying major subjects in the report.

Block 15. Number of Pages. Enter the total number of pages.

Block 16. Price Code. Enter appropriate price code *(NTIS only)*.

Blocks 17. - 19. Security Classifications. Self-explanatory. Enter U.S. Security Classification in accordance with U.S. Security Regulations (i.e., UNCLASSIFIED). If form contains classified information, stamp classification on the top and bottom of the page.

Block 20. Limitation of Abstract. This block must be completed to assign a limitation to the abstract. Enter either UL (unlimited) or SAR (same as report). An entry in this block is necessary if the abstract is to be limited. If blank, the abstract is assumed to be unlimited.

FOREWORD

Opinions, interpretations, conclusions and recommendations are those of the author and are not necessarily endorsed by the US Army.

____ Where copyrighted material is quoted, permission has been obtained to use such material.

____ Where material from documents designated for limited distribution is quoted, permission has been obtained to use the material.

____ Citations of commercial organizations and trade names in this report do not constitute an official Department of Army endorsement or approval of the products or services of these organizations.

____ In conducting research using animals, the investigator(s) adhered to the "Guide for the Care and Use of Laboratory Animals," prepared by the Committee on Care and Use of Laboratory Animals of the Institute of Laboratory Resources, National Research Council (NIH Publication No. 86-23, Revised 1985).

____ For the protection of human subjects, the investigator(s) adhered to policies of applicable Federal Law 45 CFR 46.

____ In conducting research utilizing recombinant DNA technology, the investigator(s) adhered to current guidelines promulgated by the National Institutes of Health.

____ In the conduct of research utilizing recombinant DNA, the investigator(s) adhered to the NIH Guidelines for Research Involving Recombinant DNA Molecules.

____ In the conduct of research involving hazardous organisms, the investigator(s) adhered to the CDC-NIH Guide for Biosafety in Microbiological and Biomedical Laboratories.

PI - Signature 6/1/96 Date

Perimetric Mapping of Hyperacuity:

Effects of retinal laser scars --

Midterm Report (1 year)

Elmar T. Schmeisser, Ph.D.

Table of Contents

Perimetric Mapping of Hyperacuity:

Effects of retinal laser scars --

Midterm Report (1 year)

Elmar T. Schmeisser, Ph.D.

Associate Professor

Department of Ophthalmology

801 Rose St., Room E-318

Lexington, KY 40536

Telephone:(606)233-6730

FAX: (606)257-6718

E-Mail: oph001@pop.uky.edu

INTRODUCTION:

Visual compromise due to retinal burns caused by laser exposure is well documented both in the clinical literature and in accident reports.[1-3] These have been summarized, and their effects on visual acuity and visual field tabulated.[4] While this tabulation is useful, the ranges of visual deficit for a particular estimated exposure type are extremely wide and are therefore of limited predictive value. In clinical treatment texts, effects of laser treatment are focused on the diseased tissue, and effects on the remaining retina are usually relegated to a small chapter on "complications".[5] These complications are usually dominated by a discussion of hemorrhage, with a mention of foveal coagulation. Admittedly, the clinical endpoint is the arresting of a retinal disease effect and the retention of useful

vision, but even the treating physician cannot know if the final best corrected visual acuity of his patient will be 20/40, with which the patient can drive a car, or 20/200, in which case the patient fulfills one of the criteria for legal blindness.[6]

In a military context, personnel operating in a directed energy warfare (DEW) battlefield may be subject to hostile targeting by not only laser rangefinders and designators, but also by weapons systems specifically using these modalities in an attempt to compromise mission performance. Since weapons systems aiming involves predominantly a vernier acuity task (aligning crosshairs or front with rear weapon sights), this ability is critical in the military and directly affects return to duty status, i.e. aiming a weapon accurately requires functional hyperacuity. With a compromise in the ability to detect small offsets between visual items (i.e. front with rear sights and the target), aiming effectiveness and thus weapons effectiveness must decrease. Any personnel using optical sighting devices, whether on the ground, onboard ships or airborne, are at risk. Additionally, both field commanders as well as military medical personnel must be prepared to estimate the effect on personnel, mission and casualty triage from as strong a database as possible. The consequences of laser retinal lesions are of interest to the military medical community that must deal with the problem of laser exposures to personnel by laser rangefinders and laser target designators.[7] Experimental data is urgently needed that will bear on the effects of DEW exposures on critical visual function in high luminance environments.[8] This protocol

specifically addresses the quantification of visual effects of retinal laser lesions on high-acuity, high-luminance visual tasks that correspond with the critical military task of weapon to target alignment.

This report reports the initial efforts and results of the experiments on the ability of the visual system to make localization judgments, i.e. vernier or hyperacuity, as opposed to pattern resolution judgments, e.g. grating or letter acuities.[9] The ability of an observer to correctly judge the offset of 2 dots or line elements is quite resistant to optical degradation and is significantly different in its response to pathology.[10-12] Visual evoked potential correlates of hyperacuity have been obtained in humans as well.[13-16] These studies show that hyperacuity VEP scales linearly with log offset and thus permits accurate determination of the psychophysical hyperacuity threshold by extrapolation to signal amplitude extinction. The key question addressed by this protocol is: to what extent do retinal laser exposures (which produce changes from minimally visible retinal lesion levels up to and exceeding clinical treatment level burns) near and on the fovea affect both vernier acuity and grating resolution?

The secondary question posed in the original proposal was: can the scotoma resulting from laser burns be mapped objectively, i.e. by neural response? Various forms of electrophysiological perimetry have been attempted in the past, but the method that seems of greatest promise is that developed by Suter et al.[17] In

this method, an entire stimulus array of hexagons is presented at once covering up to 30 degrees of visual angle. Each hexagon within the array has its own unique on/off pattern, and all hexagons have their on/off patterns interleaved simultaneously in an m-sequence such that the recorded signal can have each hexagon's contribution separately extracted. The result is a map of local signal response as a function of perimetric location. the data acquisition can take up to 15 or more minutes; however, since all elements are active at once, any instability in the recording situation is reflected across the entire session rather than leading to trend errors. The hypothesis proposed is that this method can be sufficiently sensitive to detect and quantitate minimal visible lesions (MVL) reliably in these animals.

Methods:

Subjects: The decision of a suitable species was driven by 3 considerations: the animal must be a primate, it must have high luminance, high acuity color vision, and its retina must have a fovea. These requirements arose from the need to model the human visual system organization (anatomy and function) both retinally and cortically in order to generalize the results of this study to human visual performance. The lowest species therefore that could be used was the cynomolgus monkey (Macaca fascicularis). The animals in this protocol have already had the requisite lesions placed as follows: graded laser lesions had been produced by the native collimated beam from a pulsed laser emitting 1062

nm light without expansion or focusing by any lens system other than that of the eye itself. Placement and severity of lesions was governed by attempts to produce "Wolfe grade" equivalent effects[4] with a single Q-switched exposure. Four exposures had been placed in one eye of each animal, the other eye serving as a normalizing control with no laser exposures (see Table 1, below). The acute effects of these exposures on acuity as measured by the sweep VEP technique have been previously reported.[18,19]

TABLE 1: RETINAL LESION PATTERN

	LOCUS:			
	SUP	TEMP	INF	FOV
MONKEY:				
1	IA	IIA	IIIA	IB
2	IIA	IIIA	IA	IB
3	IIIA	IA	IIA	IB
4	IA	IIA	IIIA	IIB
5	IIA	IIIA	IA	IIB
6	IIIA	IA	IIA	IIB
7	IA	IIA	IIIA	IIIB
8	IIA	IIIA	IA	IIIB
9	IIIA	IA	IIA	IIIB

DEFINITIONS:[4]

I: EDEMA/MIN BURN (ED50 B)

II: BURN/NECROSIS (ED90 B)

III: MIN RET HEMM (ED50 H)

A: 5 DEGREE ECCENTRICITY

B: FOVEAL (0 DEGREES)

(note: animal #5 died due to other medical causes (1989); animal #6 has just been terminated due to untreatable diabetes and cataracts)

Stimulus: The hyperacuity (vernier) stimuli were produced on a high resolution monochrome monitor placed at 2 meters from the animal. The stimulus pattern was modulated under computer control to produce high illuminance (greater than 2 log-trolands) stimuli. The stimuli are split bars whose segments can be horizontally offset. The offset was counterphased between 0 and some number of pixels to evoke a VEP. The stimulus parameter size (i.e. the number of pixels offset) was varied and the visual system response recorded. Also, a checkerboard pattern was varied in size to give an estimate of the animal's visual acuity (see Recording, below). The perimetric mapping stimuli were produced on a high resolution color monitor placed at 800 cm from the animal, and run by a second system that controlled both the stimulus and the data acquisition from the same hospital grade amplifiers used by the vernier system.

Recording: In general, the steady-state pattern VEP was recorded from the scalp electrodes in response to the stimulus. For the hyperacuity measures, a regression between log bar offset and VEP response strength defines the vernier threshold. For the perimetric data, the ratio of the response amplitude per location in the 4 sites in the (unexposed) control eyes to the equivalent sites in the lesioned eyes should give the relative scotomata depth and extent.

Procedure: The animal was brought to the laboratory, sedated and premedicated with ketamine IM. The animal was anesthetized with Nembutal IV and muscularly relaxed with

pancuronium bromide IV. The animal was intubated and wrapped in a warming blanket. Temperature, ECG and pCO_2 were monitored; ventilation and blanket temperature was adjusted to maintain physiologic values. EEG and ECG were monitored for signs of discomfort and the anesthetic level adjusted accordingly. The animal was aligned in front of the fundus camera on a padded rotating stage and the retina visualized. For this report, only the foveal sites were examined. Steady-state VEPs (vernier or resolution stimuli), or mapping recordings also were taken from the unexposed eye for comparison.

After an experimental session, the animal was allowed to recover from both the muscular immobilizing agent and the anesthetic. When it could breathe unassisted, it was extubated, removed to the transfer cage and then be returned to the colony under the supervision of the veterinary staff.

Results to date:

Physical recording: The initial optical layout has been altered to remove all optics other than the shielded window from between the animal's eye and the stimulus screen. Following an initial series of recordings of the experimental eyes (see below), it was determined that both eyes would have to be available in a single session. Therefore, the fundus camera mounting system was again rebuilt to permit viewing of both eyes. This has revealed a between 5 and 10 degree esotropia in various animals while under sedation. However, it also has resulted in some problems with the larger male animals by physical

interference with their more prominent brow ridges. These 4 large animals were recorded from before this rebuild, and have the more severe ("red dot": contained retinal hemorrhage) foveal lesions. The smaller animals with lesser lesions are easily accommodated in the new arrangement. The vernier stimuli are presented on a monitor at 21 meters distance, while those for the mapping study are presented at 800 cm distance (20 degree diameter field).

Vernier acuity results: Programming of the acquisition system proved more complex than expected. The objective was to find the smallest possible stimulus image that would permit useful analysis; such a stimulus would permit the greatest possible localizing of the lesion extent and the least amount of response contamination by normal neighboring retina. Initial attempts using a single split vertical bar failed to give reliable VEPs. Finally, the stimulus system had to be reconfigured to accept 2 1024 by 1024 pixel pcx graphics files as the stimulus images to alternate between. This permitted the presentation of any arbitrary pattern and was not constrained by the programming of the stimulator. Initial runs were with a stimulus defined in papers describing oscillatory displacement threshold testing in human patient populations. VEPs acquired with such a stimulus were disappointing in that the signal was too small to be reliably resolved from the background noise. The next stimulus set to be attempted was a single line alternating between broken and unbroken states. This also was unsuccessful. After an extensive series of different pattern attempts,

reasonable response recording was obtained with a vertical series of 5 bars, of which the central one third segment was horizontally offset (Fig 1). Comparison recordings with a human volunteer were made with the same stimulus to validate the identification of the response waveform (Fig. 2). This reconfiguration initially resulted in the loss of the slaved trigger signal from the stimulator. However, the image exchange can be externally triggered (one trigger for 2 frames), which the acquisition program could initiate via a programmable pulse, simplifying control. Several experiments were run with the larger animals that had red dot lesions in the fovea, as noted above. Threshold VEP acuity (to checkerboards) was uniformly extremely poor (approximately 1 cycle/degree) and vernier acuity was not measurable in these animals. However, recordings from the normal eye were not optimal, either. The tentative conclusion is that vernier acuity is not preferentially spared in cases of severe resolution acuity loss due to damage, unlike cases where such resolution loss is due to media changes (corneal clouding, lenticular cataract, etc.). Experiments are continuing in animals with less severe lesions and better preserved acuity. These animals may show differential effects between resolution and vernier acuities, and can be used to determine the range of normal variation in the responses.

Electrophysiological function mapping results: Initial VEP mapping experiments used the Suter multi-input stimulus system to examine the visual field. The Suter system is sensitive to both numeric overflow and underflow conditions, and does not warn the

user of these artefactual conditions. Consultation with Dr. Suter has resolved some of these issues. The project was modified to attempt the mapping by the better characterized ERG (retinal) responses first. Work on this protocol objective has proceeded slowly. Problems include very high variability in the resulting maps and an apparent non-monotonic relationship between visible lesion characteristics and signal decrements in the retina. Preliminary results were presented at the SPIE meetings in San Jose at the end of January, 1996 in the laser bioeffects session. Proceedings are to be published which will include these data (see Appendix A for detailed methods and the preliminary results that were presented). In order to record both eyes simultaneously (the experimental and the control), the mapping stimuli may have to be unscaled (i.e. all hexagons equal in size) so that the two eyes will have comparable stimuli no matter what the animal's esotropia. The stimulus distance has also been altered so as to include the entire retinal area of interest (the central 20 degrees) within one map for the future recordings.

As of May, one animal (number 6, noted earlier) developed an acute, uncontrollable case of non insulin dependent diabetes and subsequent severe cataracts. These cataracts made this animal unsuitable for this study. The animal was terminated, the eyes enucleated and fixed for histology. Recovery of the lesions from this retina will be done at the Medical Research Detachment (WRAIR), Brooks AFB, Texas following delivery of the fixed tissue. As noted above, an earlier animal (#5) died shortly

after completion of the acute protocol in 1989; however, the eyes from that animal were also retained and have been fixed and sectioned for study. These slides also will be sent to San Antonio. Photographic documentation of the animals' retinas has been completed (see Appendix B; graphics interchange format - GIF - images are available from the author by e-mail attachment via MIME encoding). These images will be used to overlay the retinal function maps for direct correlation between lesions and response profiles. Retinal maps of these eyes have not been consistent to date. The data is being exchanged with the system developers in order to determine the reasons for this.

Discussion and future directions:

While it is extremely difficult to "prove" a negative finding, especially with partial and non optimal data, some trends do appear. First, since vernier acuity drops off more rapidly than resolution acuity, the fovea is probably the only place to measure vernier acuity in a behaviorally relevant manner. As noted in the results section, if the resolution acuity is degraded due to actual physical disruption of the foveal area, the vernier acuity is not preferentially spared, in distinction to the effect of simple optical blurring. This finding correlates well with clinical experience since the vernier acuity is used clinically to differentiate neural losses from optical losses in the cases of compromised optical media (cataracts, etc.) Nevertheless, should the vernier VEP signals remain too small (probably due to skull thickness in the primate

when compared to actual amount of cortex responding), invasive electrodes (e.g. transcortical bipolar chronically implanted wires) may be required to get an acceptable signal/noise ratio. This type of method would require a new application to the institutional IACUC and additional separate approval from the contract managers since it involves survival surgery and additional expense. The drawback of this method is that a single set of electrodes may miss the appropriate patch of cortex. An alternative is to implant a rectangular array or grid of pins over each visual cortex, allowing the experimenter to select the appropriate recording area at hoc. The final alternative would be nonsurvival surgery, recording acutely from an opened skull, and exploring for the signal on the exposed cortical surface. The obvious disadvantage is that this is a single opportunity attempt with no margin for either error or repeated acquisitions.

The mapping studies are currently plagued with two problems: very small signal sizes and baseline instability in the signal. The small signal sizes may be unavoidable since high resolution (and correspondingly small stimulus areas) are desired, and the fact that the animal has a smaller retina (less neural tissue) responding than the human. The signal instability is currently being addressed by exploring alternate recording electrodes and recording montages. The most promising to date has been an inter-ocular recording method using foil electrodes. In this method, the fellow eye acts as the reference electrode, and is occluded so as to receive no stimulus. Since the amplifiers have a large common mode rejection ratio, all system instabilities

should cancel each other out. The drawback from this technique is that far field potential differences may interfere. If this method fails, specialty bipolar Burian Allen style lenses may have to be manufactured for the animals.

References:

1. Moshos M. ERG and VER findings after laser photocoagulation of the retina. Metab Pediatr Ophthalmol 6:101 (1982).

2. Fowler BJ. Accidental industrial laser burn of the macula. Ann Ophthalmol 15:481 (1983).

3. Boldrey EE, Litle HL, Flocks M, Vassiliadis A. Retinal injury due to industrial laser burns. Ophthalmol (Rochester) 88:101 (1981).

4. Wolfe JA. Laser retinal injury. Mil Med 150:177 (1985).

5. Zweng HC, Little HL, Vassiliades A. Argon laser photocoagulation. Publ CV Mosby Co. St. Louis , p 292 (1977).

6. American Medical Association. Guides to the evaluation of permanent impairment (2nd edition). AMA, Chicago, IL. Pages 141-152 (1984).

7. Taken from an anonymous outside reviewer's comments on a related protocol (1988).

8. American National Standards Institute. Safe use of lasers, ANSI Z - 136.1 - 1980. New York: American National Standards Institute (1980).

9. Westheimer G. Visual acuity and hyperacuity: resolution, localization, form. Am J Optom Physiol Opt 64:567-574 (1987).

10. Enoch JM, Williams RA. Development of clinical tests of vision: Initial data on two hyperacuity paradigms. Percept Psychophys 33:314-322 (1983).

11. Enoch JM, Essock EA, Williams RA. Relating vernier acuity and Snellen acuity in specific clinical populations. Doc Ophthalmol 58:71-77 (1984).

12. Enoch JM, Williams RA, Essock EA, Barricks M. Hyperacuity perimetry. Assessment of macular function through ocular opacities. Arch Ophthalmol 102:1164-1168 (1984).

13. Levi DM, Manny RE, Klein SA, Steinman SB. Electrophysiological correlates of hyperacuity in the human visual cortex. Nature 306:468-470 (1983).

14. Steinman SB, Levi DM, Klein SA, Manny RE. Selectivity of the evoked potential for vernier offset. Vis Res 25:951-961 (1985).

15. Srebro R, Osetinsky MV. The localization of cortical activity evoked by vernier offset. Vis Res 27:1387-1390 (1987).

16. Tyler CW, Apkarian P, Levi DM, Nakayama K. Rapid assessment of visual function: an electronic sweep technique for the pattern visual evoked potential. Invest Ophthalmol Vis Sci 18:703 (1979).

17. Bearse, MA Jr, Suter EE. Imaging localized retinal dysfunction with the multifocal electroretinogram. J Opt Soc Am A 13:634 (1996).

18. Schmeisser ET. Laser lesion effects on acute visual functions I. Grating visual acuity by sweep VEP. Final report on Contract # F33615-88-C-0631, P.O.# 21582, submitted to the USAF School of Aerospace Medicine, Brooks AFB, TX.

19. Schmeisser ET. Acute laser lesion effects on acuity sweep VEPs. Invest Ophthalmol Vis Sci, 33:3546-3554, (1992).

Appendix A:

Copy of the manuscript for the
SPIE meetings reporting preliminary
results from the retinal mapping studies

Evaluation of retinal laser lesion healing by perimetric electroretinography

Elmar T. Schmeisser

Dept. of Ophthalmology, E-318 Kentucky Clinic,
University of Kentucky, Lexington, KY 40536-0284

ABSTRACT

Eight Cynomolgus fasciculata who had graded laser lesions placed in one eye 6 years previously were evaluated by a stimulation and electrophysiologic recording technique to produce maps of retinal function. All animal testing was performed under IACUC approved protocols. The single q-switched pulses from a neodymium-YAG laser produced lesions of 4 types: no visible change, minimal visible lesions, "white dot" lesions (localized circumscribed retinal blanching) and "red dot" lesions (contained retinal hemorrhage) in the eye at the time of placement. Single exposures had been made in four locations: 5 degrees superior, inferior and temporal to the fovea, and one foveally. The multifocal (perimetric) electroretinogram was recorded from specialized contact lenses through hospital grade amplifiers. Initial analyses gave field maps that demonstrated apparent relative loss of function in some lesion sites. However, these losses were variable and occasionally patchy (i.e. disconnected areas of low signal). Repeated examinations of the same retinal areas showed high variability, even with 15 minute acquisition times and no apparent gaze drift. Apparent losses did not appear to correlate with visible retinal changes at the lesion site. Further research is needed to determine the biological substrate for this variability in response topography.

Keywords: damage, electroretinogram, laser, neodymium, perimetry, primate, retina, q-switch, Wolfe grade.

1. INTRODUCTION

Visual compromise due to retinal burns caused by laser exposure is well documented both in the clinical literature and in accident reports.[1-3] These have been summarized, and their effects on visual acuity and visual field tabulated.[4] While this tabulation is useful, the ranges of visual deficit for a particular estimated exposure type are extremely wide and are therefore of limited predictive value. In clinical treatment texts, effects of laser treatment are focused on the diseased tissue, and effects on the remaining retina are usually relegated to a small chapter on "complications".[5] These complications are usually dominated by a discussion of hemorrhage, with a mention of foveal coagulation. Admittedly, the clinical endpoint is the arresting of a retinal disease effect and the retention of useful vision, but even the treating physician cannot know if the final best corrected visual acuity of his patient will be 20/40, with which the patient can drive a car, or 20/200, in which case the patient fulfills one of the criteria for legal blindness.[6]

Histological and anatomic studies predominantly in primates have related laser wavelength, pulse duration and energy to retinal lesion size and depth.[7-9] Based on

these changes, and on maps of normal visual acuity vs retinal eccentricity,[10] inferences are made about the functional defects in that detectable lesions imply a loss of function. While there is general agreement about the histology of laser lesions in the retina, the visual correlates of these lesions are still unclear. Behavioral assays in primates have also showed conflicting results with foveal lesions.[11,12] Since the visual system of the monkey has been shown histologically, anatomically, electrophysiologically and, within certain constraints, psychophysically to parallel the human.[3,14] The electrophysiological to perceptual correlate is well established in humans with both averaging and vector-voltmeter techniques.[15,16] In an attempt to circumvent the problems of psychophysical research in animals, more direct assays of neural function have been attempted, but since lesions are inherently irreversible, averaging techniques can not be employed. The result has been that retinal burns have produced effects on the signal that could not easily be related to visual function.[17]

Previous studies by the author have examined the effects of laser exposures on the electrophysiological function of circumscribed areas of the retina. This was accomplished by recording the visual evoked potential (VEP) from scalp electrodes.[18-20] While this montage samples the entire central retina, averaging was required to extract the low signal. Use of implanted bipolar cortical electrodes in further studies allowed single exposure evaluation.[21,22] However, these electrodes have "receptive fields" of only 1 to 2 degrees in diameter. While the pattern electroretinogram (ERG) has also been recorded, thus sampling the entire macular area,[23] the signal to noise level as well as the standard stimulus and recording systems currently being employed do not permit precise measurement of the local functional changes in the retina in and around small lesions.

Recently, an innovative experimental technique has been developed that may address this problem: multi-input electroretinography.[24] This method uses a tiled display in which each hexagonal tile is flickered independently such that the overall averaged luminance change is zero and each tile has a unique temporal signature (m-sequence). The ERG is recorded to this multiple stimulus from a single recording electrode and then cross-correlated to each tile's individual signature. This results in a topographic or perimetric map of the retinal response which seems to correlate with ganglion cell density across the retina. The technique is just beginning to be applied to selected patients with clinical retinal disease, but should be able to resolve damage from focal laser lesions as well. If this method demonstrates sufficient sensitivity, and can be shown to correlate with functional changes (e.g. acuity, contrast sensitivity), a powerful objective method for predicting the functional consequences of anatomically visible lesions will become available. This paper reports a test of this method in primates who have had laser lesions placed in their retinas from known exposure energies.

2. METHODS

2.1 Subjects The decision of a suitable species is driven by 3 considerations: the animal must be a primate, it must have high luminance, high acuity color vision, and its retina must have a fovea. These requirements arise from the need to model the human visual system organization (anatomy and function) both retinally and cortically in order to generalize the results of this study to human visual performance. The lowest species that would therefore be used was the cynomolgus

monkey (Macaca fascicularis). Further, the recording methods are noninvasive and routinely used with human patients. All procedures were pre-approved by the university IACUC and followed the guidelines of both ARVO and the NIH.

Graded laser lesions had been placed 6 years previously by the native collimated beam from a pulsed Nd-YAG laser emitting 1062 nm light without expansion or focusing by any lens system other than that of the eye itself. Placement and severity of these lesions was governed by attempts to produce "Wolfe grade" equivalent effects[4,25] with single Q-switched exposures. Four lesions had been placed in one eye of each animal, the other eye serving as a normalizing control with no laser exposures. The exposure energy (and thus lesion type) was counterbalanced across both locations and animals for severity and only four exposures were made in the right eye of each animal. The left eye remained as an unexposed control. The acute effects of these lesions on acuity as measured by the sweep VEP technique have been previously reported.[26]

Figure 1 shows the a coded schematic of the resulting lesions labeled at the time of placement. Summarizing the 8 animals remaining, at the foveal site there are 2 remaining who were labeled with no visible change at the time of exposure, 2 with a "minimal visible lesion" (MVL, or Wolfe Grade 1B), 2 with white dot lesions (IIB) and 3 with red dot lesions (IIIB). At the parafoveal locations, there are 11 sites with no visible change at the time of exposure, 4 sites with MVL (IA), 6 sites with a white dot lesion (IIA), and 4 sites with a red dot lesion (IIIA). One animal is no longer alive, but the eyes were preserved for later histological analysis of its lesion sites (results to be reported elsewhere).

2.2 Stimulus and Recording The stimulus was produced by a specially designed Nu-Bus video board hosted in a Macintosh Quadra 650 computer. Two multi-sync monitors are attached (one 14 inch stimulus monitor and one console monitor) and data was acquired by an analog to digital converter also housed in the same computer. The raw signal was recorded from corneal contact lens electrodes and preamplified with hospital grade amplifiers before being fed to the computer. Amplifiers were set to a gain of 100,000 with a bandpass of 3 - 100 Hz. The specially written software package (VERIS^{tm}) simultaneously updates multiple areas on the stimulus monitor while synchronously acquiring the electrophysiological data and calculating the next m-sequence set. This system is available from the developer, Dr. Erich Sutter (Smith-Kettlewell Eye Research Institute, 2232 Webster St., San Francisco, CA 94115).

Parafoveal sites were mapped with a 61 element, equal area hexagonal stimulus pattern placed at 1 meter distance. The foveal sites were mapped with a similar pattern that was size scaled so that each hexagon would produce approximately equal amplitude responses, i.e. the central hexagons were smaller than the peripheral ones. The arrangement resulted in approximately 1 degree resolution in the 8 degree perimetric maps without interpolation.

2.3 Procedure The animal was brought to the laboratory, sedated and premedicated with ketamine IM. The animal was anesthetized with Nembutal IV (10 mg/kg) and muscularly relaxed with pancuronium bromide IV (0.025 mg/kg) as bolus doses. The animal then was intubated and wrapped in a warming blanket. Temperature, ECG and pCO2 was monitored; ventilation and blanket temperature were adjusted to maintain physiologic values. EEG and ECG were monitored for signs of discomfort and the

anesthetic level adjusted with backup doses as needed. The animal was aligned in front of the fundus camera on a padded rotating stage. The ERG contact lens electrode was placed on the cornea over artificial tears and the retina visualized through it. Figure 2 shows the optical layout and alignment system.[27] One site in one eye was selected for examination per day. Mapping ERGs were taken on separate days centered on each lesion of the exposed eye. Each map was calculated from a 15 min long m-sequence acquisition. At least 2 maps were made at each site to evaluate signal variability. For this report, 3 foveal and 2 peripheral lesions were evaluated: for the foveal site, one each of no effect, minimally visible lesions (MVL) and white dot in 3 animals; for the parafoveal locations: white dot lesions for 5 degrees inferior and for 5 degrees temporal in 2 different animals.

After an experimental session, the animal was allowed to recover from the muscular immobilizing agent. When it could breathe unassisted, it was extubated, removed to the transfer cage and then returned to the colony under the supervision of the veterinary staff.

RESULTS

The initial map was constructed for the 5 degree inferior location that was noted to have a white dot lesion when the retina was exposed 6 years earlier (trace array in Fig. 3, grey scale map in Fig. 4). In order to determine what the signal itself looked like, an overall sum was created from all responses in the map (Fig. 5). The resulting waveform had the general conformation of an ERG with an a-wave and a b-wave, and was slightly delayed as compared to human normal recordings with the same machine (i.e. b-wave peak near 45 msec). From the trace array, a horizontal profile was constructed from the row of responses just above the centerline (Fig. 6). This profile shows a marked drop in response in 3 paracentral fields, indicating an approximately 2 degree scotoma (the open square is shown twice: once on the left half and once on the right half of the plot). The vertical meridian through the same locus showed only a single reduced point, implying that the apparent lesion had almost a 3:1 asymmetry.

Another map was constructed from a second animal with a similar lesion 5 degrees temporally. In this animal, despite similar visible scarring in the retina, the response profile was extremely variable, showing very patchy and disconnected areas of dropout several degrees eccentric to the visible lesion (centered on the stimulus pattern) that dropped to only 25% of the map maximum amplitude (profile in Fig. 7).

Maps from the 3 animals with foveal exposures (one with an MVL and the other with a white dot lesion) showed a signal maximum near the center of the stimulus pattern on separate maps. The animal with no visible change upon exposure, however, did not show the same stimulus response pattern with repeat testing. Repeat mapping in this animal showed that the "hot spot" seemed to have moved 2 hexagons away. Nor was the overall pattern between the two maps similar in either amplitude distribution or overall response level. Combining these maps to improve the signal to noise ratio resulted in the creation of a new hot spot not seen in either component map. The map from the foveal MVL animal showed an apparently deeper scotoma than the map from the white dot lesioned animal.

DISCUSSION

Clinical use of the multifocal ERG technique has produced waveforms that appear similar to classical flash ERG waveforms in shape and timing, i.e. a triphasic waveform with the apparent cornea positive b-wave peak occurring near 40 msec. This waveform has therefore been labeled as an "ERG" since it is recorded from a contact lens electrode on the cornea in response to (many local) luminance changes. Recent reports on a patient with a local branch retinal vein occlusion (BRVO) in an eye has raised some doubts whether the recorded signal is in fact an ERG.[28] In BRVO, the standard flash evoked ERG demonstrates a negative form in which the positive deflection (the b-wave) is reduced and the leading negative deflection (the a-wave) is enhanced in the affected areas. Clinically, this is expressed as the fact that the a-wave to b-wave amplitude ratio drops below 1.0 (normally near 1.8 or greater). This ratio shift results from the loss of middle and inner retinal perfusion, leaving only the outer (photoreceptor elements) active. With the multifocal ERG technique, such a dramatic wave shape alteration was not found, although an overall response reduction was observed in the affected retinal areas.

As noted in the results, maps of the foveal zone in the animal with no visible changes following a low level laser exposure 6 years previous (and which showed no acute alterations in VEP acuity at the time) were not repeatable, with the apparent foveolar maximum response shifting several hexagons each run. This might imply that the eyeball had drifted (moved) during the 15 minute run, despite the immobilizing agent. If so, this drift would have been of at least 2 degrees and was not apparent through the fundus camera alignment system. More importantly, the overall pattern of response itself did not shift as a unit, i.e. was not repeatable, with patches of response dropout appearing apparently randomly on the two maps as well as large shifts in apparent topography. This may indicate that either the signal might have been too small (underflow) or that the stimulus areas were insufficient to evoke an stable response (e.g. smaller than some postulated minimum stimulus field size needed to produce an ERG). However, summation of the overall signal indicated an mean amplitude almost identical to the developer provided normal human signals implying that signal underflow was not occurring. It might be noted that the timing (of 45 msec to the b-wave peak) is normally seen only with dark adapted retinas in response to bright light flashes, while these recordings were made in photopic conditions. Normal photopic ERGs have faster b-wave timings generally below 30 msec, while pattern ERGs are slower (positivity at 50 msec).

Taken together, these results imply that the signal being recorded is not an ERG in the sense normally meant. Further research is needed to determine the biological substrate for these signals' variability and wave shape as they do not appear to correspond with classically recorded luminance or pattern electroretinograms in the same species. This should not prevent the use of this technique to map appropriate response losses, but may place constraints on the interpretation of the results, e.g. which cell types or layers are most affected.

The number of lesion sites investigated to date include only a sample of those that are available in these animals. From these few sites, it seems that the obvious visible measures of the lesions (none, minimal, and white dot) did not correlate in a monotonic fashion with the apparent scotomas as measured by the multifocal ERG, nor did the three white dot lesions have similar maps. Whether this reflects a nonuniformity in the retinal response to the laser exposure or partial

and variable recoveries across time in the lesioned areas with and/or between animals is an open question. Further data from fluorescein and indo-cyanin green angiography as well as confocal scanning laser ophthalmoscopy to characterize the perfusion and physical parameters of the lesion sites may provide better correlation to the functional changes noted by multifocal electroretinography than simply the physical appearance of the lesion sites at the time of exposure.

Since this research is still ongoing, it can only be concluded at this point that the multifocal ERG technique has theoretical promise for this application, but may not yet be sufficiently robust to be used for fine detail mapping of the retinal response profile when used in the conditions reported above. Coarser grain stimulus patterns, either by reducing the eye to stimulus distance or using maps with larger hexagons may resolve the current difficulties.

ACKNOWLEDGEMENTS

This work was supported in part by funds under USAMRMC Contract No. DAMD17-95-C-5038, Ft. Detrick, MD, by funds from Armstrong Laboratories, Brooks AFB, TX, and by an unrestricted departmental grant from Research to Prevent Blindness, Inc.

REFERENCES

1. Moshos M. ERG and VER findings after laser photocoagulation of the retina. Metab Pediatr Ophthalmol 6:101 (1982).

2. Fowler BJ. Accidental industrial laser burn of the macula. Ann Ophthalmol 15:481 (1983).

3. Boldrey EE, Litle HL, Flocks M, Vassiliadis A. Retinal injury due to industrial laser burns. Ophthalmol (Rochester) 88:101 (1981).

4. Wolfe JA. Laser retinal injury. Mil Med 150:177 (1985).

5. Zweng HC, Little HL, Vassiliades A. Argon laser photocoagulation. Publ CV Mosby Co. St. Louis , p 292 (1977).

6. American Medical Association. Guides to the evaluation of permanent impairment (2nd edition). AMA, Chicago, IL. Pages 141-152 (1984).

7. Stuck BE, Lund DJ, Beatrice ESW. Repetitive pulse laser data and permissible exposure limits. Presidio of San Francisco, CA: Letterman Army Institute of Research. Institute Report No. 59 (1978).

8. Gibbons WD, Allen RG. Retinal damage from suprathreshold Q-switch laser exposure. Health Phy 35:461 (1978).

9. Allen RG, Thomas SJ, Harrison RF, Zuglich JA, Blankenstein MF. Ocular effects of pulsed Nd laser radiation: variation of threshold with pulsewidth. Health Phy 49:685 (1985).

10. Mandelbaum J, Sloan LL. Peripheral Visual Acuity. Am J Ophthalmol 30:581 (1947).

11. Merigan WH, Pasternak T, Zehl D. Spatial and temporal vision in macaques after central retinal lesions. Invest Ophthalmol Vis Sci 21:17 (1981).

12. Callin GD, Devine JV, Garcia P. Visual compensatory tracking performance after exposure to flashblinding pulses: I, II, III. USAF School of Aerospace Medicine, Brooks Air Force Base, TX: Reports SAM-TR-81-3, -7, -8 (1981).

13. Riggs LA, Wooten BR. Electrical measures and psychophysical data on human vision. In: Jameson D, Hurvich LM (eds); Handbook of Sensory Physiology, Springer Verlag, New York; Vol VII/4, (1972).

14. Blough DS, Yager D. Visual Psychophysics in animals. In : Jameson D, Hurvich LM (eds); Handbook of Sensory Physiology, Springer Verlag, New York; Vol VII/4, (1972).

15. Regan D. Steady-state evoked potentials. J Opt Soc Am 67:1475 (1977).

16. Tyler CW, Apkarian P, Levi DM, Nakayama K. Rapid assessment of visual function: an electronic sweep technique for the pattern visual evoked potential. Invest Ophthalmol Vis Sci 18:703 (1979).

17. Randolph DI, Schmeisser ET, Beatrice ES. Grating visual evoked potentials in the evaluation of laser bioeffects: twenty nanosecond foveal ruby exposures. Am J Optom Physiol Opt 61:190 (1984).

18. Schmeisser ET. Flicker electroretinograms and visual evoked potentials in the evaluation of laser flash effects. Am J Optom Physiol Opt 62:35 (1985).

19. Schmeisser ET. Laser flash effects on laser speckle shift VEP. Am J Optom Physiol Opt 62:709 (1985).

20. Schmeisser ET. Laser flash effects on chromatic discrimination in monkeys. USAFSAM TR-87-17, Brooks Air Force Base, TX (1987).

21. Previc FH, Blankenstein MF, Garcia PV, Allen RG. Visual evoked potential correlates of laser flashblindness in rhesus monkeys. I. Argon laser flashes. Am J Optom Physiol Opt 62:309 (1985).

22. Previc FH, Allen RG, Blankenstein MF. Visual evoked potential correlates of laser flashblindness in rhesus monkeys. II. Doubled neodymium laser flashes. Am J Optom Physiol Opt 62:626 (1985).

23. Glickman RD, Previc FH, Cartledge RM, Schmeisser ET, Zuglich JA. Assessment of visual function following laser lesions. USAFSAM Protocol # 7757-02-82 (Contract F33615-84-C-0600) (1986).

24. Sutter EE, Tran D. The field topography of ERG components in man - I. The photopic luminance response. Vis Res 32:433 (1992).

25. American National Standards Institute. Safe use of lasers, ANSI Z - 136.1 - 1980. New York: American National Standards Institute (1980).

26. Schmeisser ET. Laser lesion effects on acute visual functions I. Grating visual acuity by sweep VEP. Final report on Contract # F33615-88-C-0631, P.O.# 21582, submitted to the USAF School of Aerospace Medicine, Brooks AFB, TX (1988).

27. Blankenstein MF, Previc FH. Approximate visual axis projection for the rhesus monkey using a fundoscope and alignment laser. Vis Res 25: 301-305, (1985).

28. Kondo M, Miyake Y, Horiguchi M, Suzuki S, Tanikawa A. Clinical evaluation of multifocal electroretinogram. Invest Ophthalmol Vis Sci 36: 2146-2150, (1995).

FIGURES

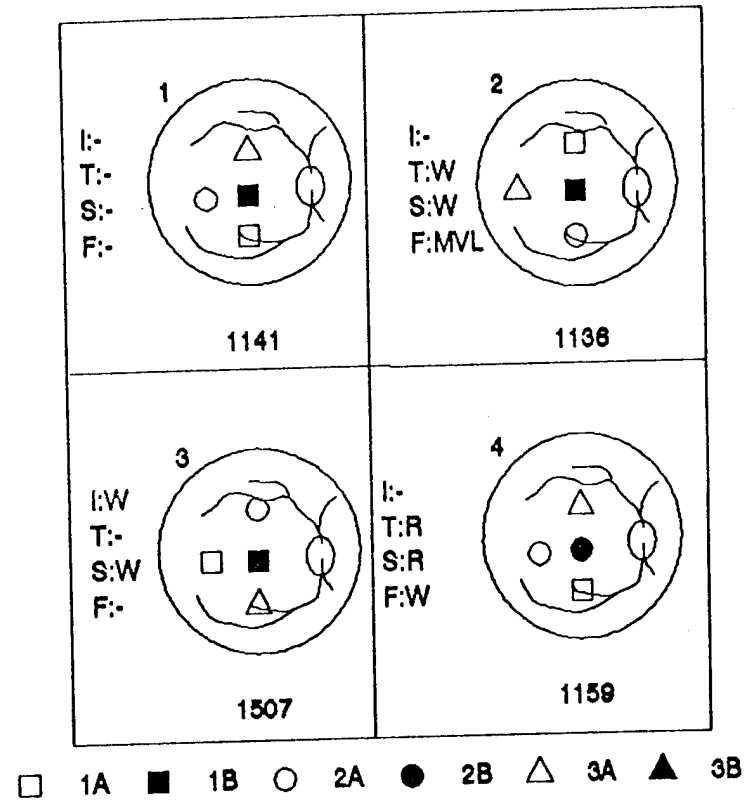

Fig.1: Schematic of the retinas from the current 4 experimental animals coded for planned exposure energy and actual resulting lesions.

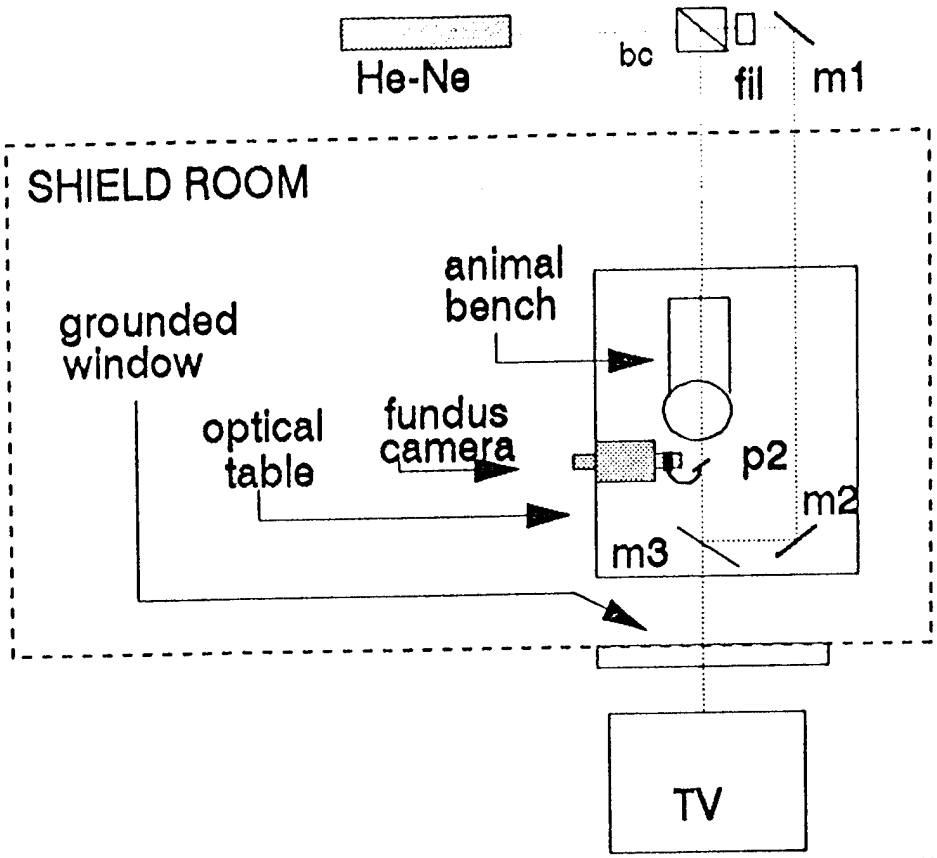

Fig.2: Layout of the optical alignment system used in this study. He-Ne: alignment laser; bc: beam splitter cube; m1, m2 & m3: mirrors (m3 can be moved from the line of sight); p2: removeable 80% reflecting pellicle.

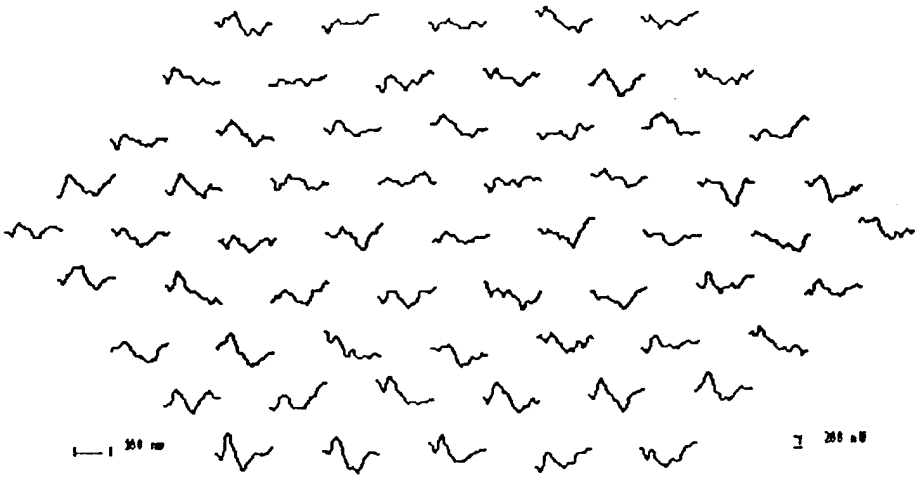

Fig.3: Trace array from CY1507 created by a 61 element equal area stimulus pattern centered at 5 degrees inferior on a white dot lesion.

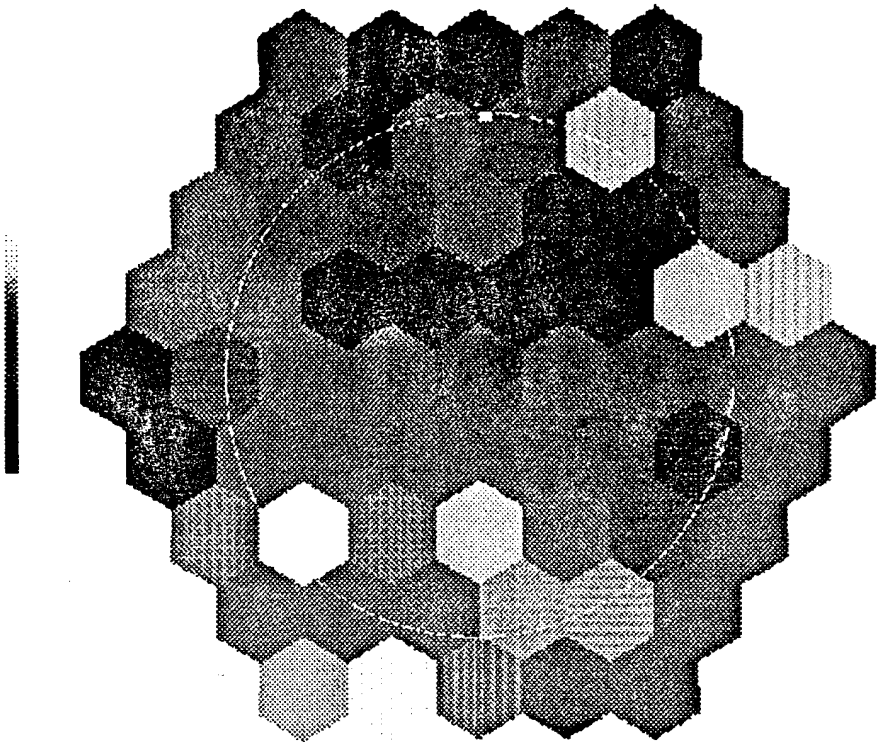

Fig.4: Grey scale map of the scalar product response metric from the trace array of fig.3. An elongated dark area of minimal to no response can be seen just above the central element.

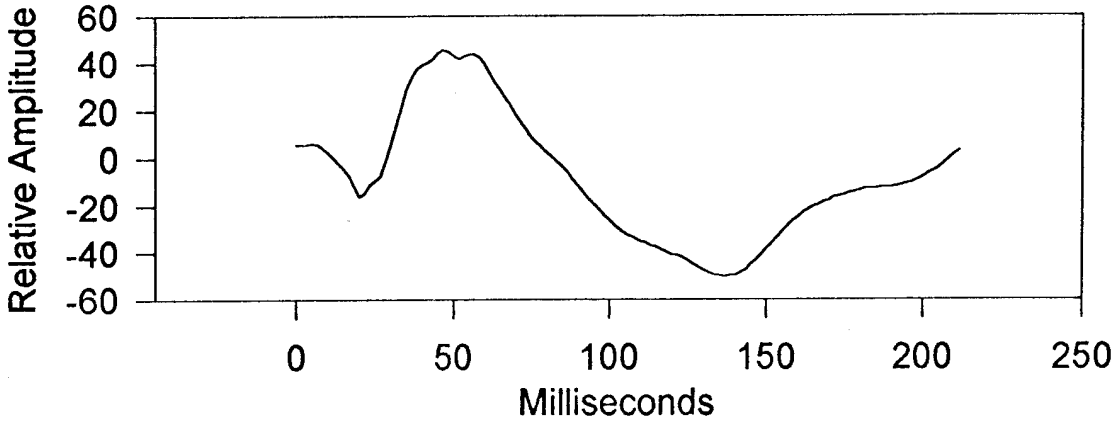

Fig.5: Overall summation of all traces from fig.3. The waveshape is comparable to human recordings in clinical settings, but delayed.

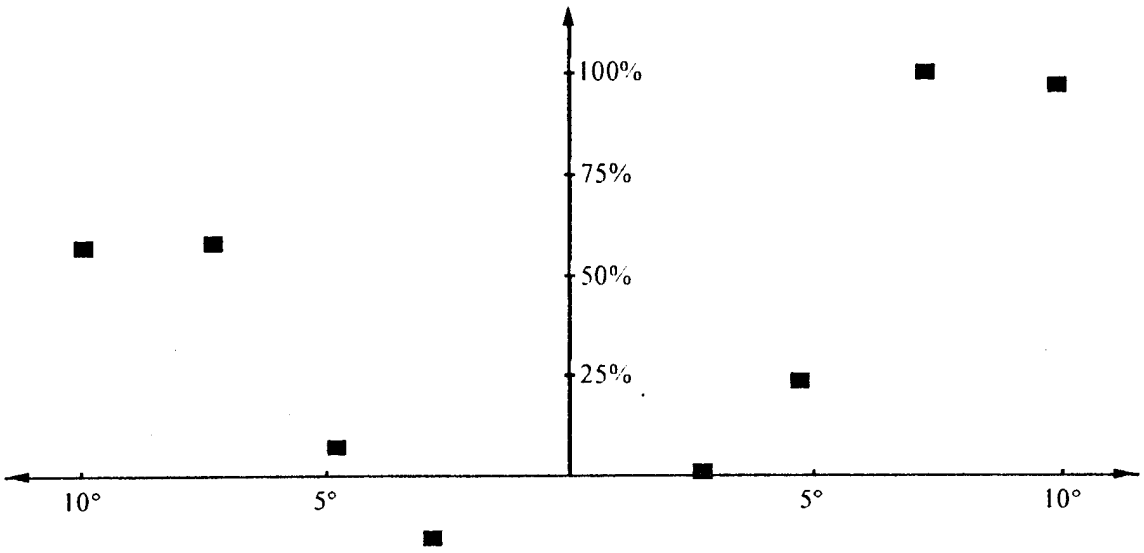

Fig.6: Horizontal profile of relative response across the horizontal band of stimulus fields just above the midline from fig. 3. A marked drop in response several sectors wide is apparent.

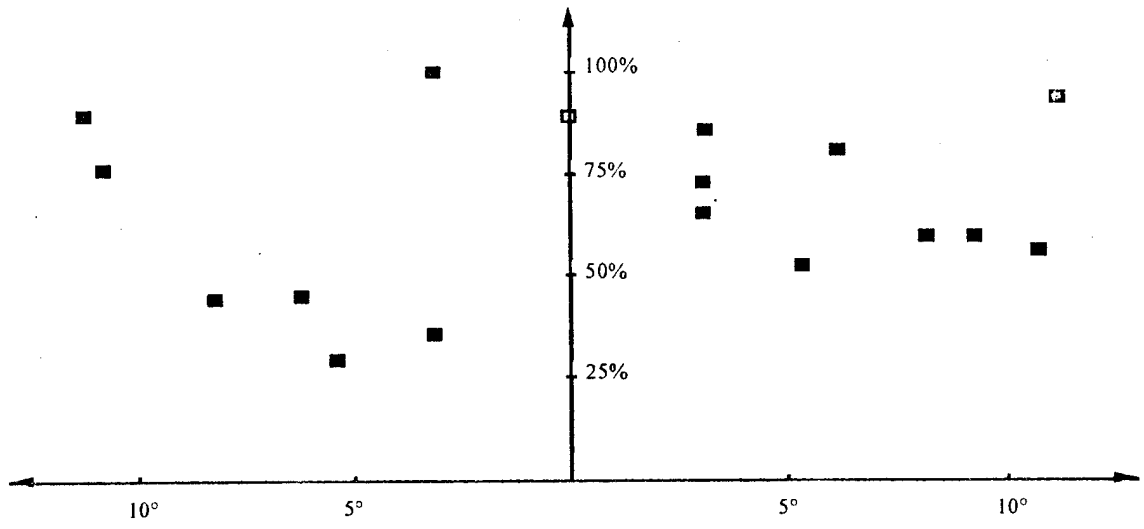

Fig.7: Vertical profile (2 hexagons wide) through the area of maximum response drop from CY1136 at 5 degrees temporal. Irregular losses of response eccentric to the apparent lesion center can be seen.

Appendix B:

Maps of the right (experimental eyes)

Fig. A1 & A2: CY 1141 OD (animal #1). At the time of exposure, no lesions were noted at any of the 4 sites, even though the superior site was targeted to receive a red-dot lesion (coded by a triangle), the temporal site a white-dot (circle) and the inferior and foveal sites an MVL (square).

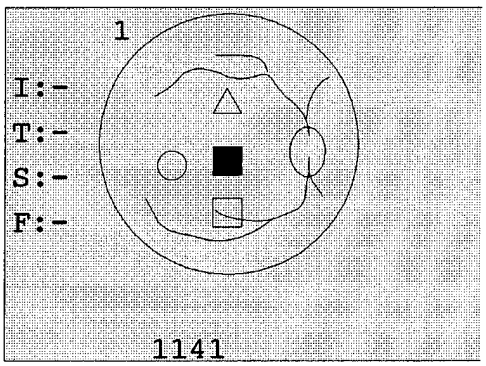

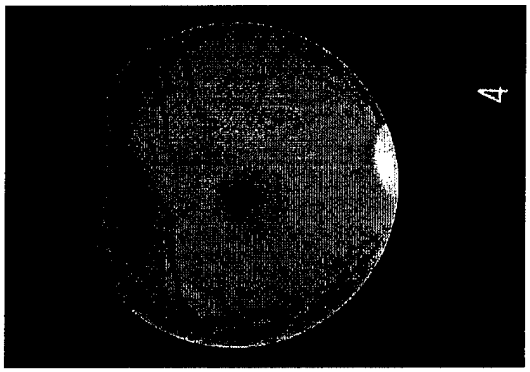

Fig. A3 & A4: CY 1136 OD (animal #2). At the time of exposure, white-dot lesions were noted both at the temporal and the superior sites. The fovea was targeted to receive a MVL, and shows a pigmentary blanching. The superior site appears at about 4 degrees, but the temporal site appears approximately 10 degrees from the fovea. Map coding (circle, triangle, square) for this and all subsequent figures is the same as above.

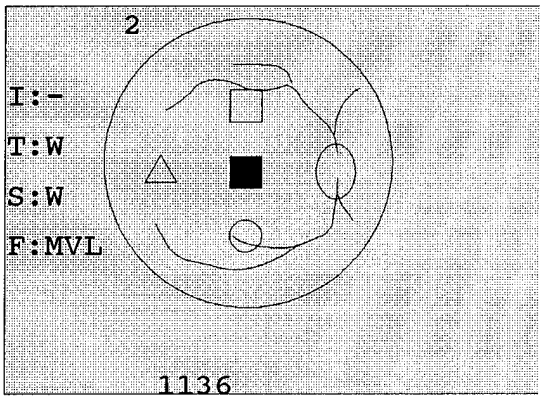

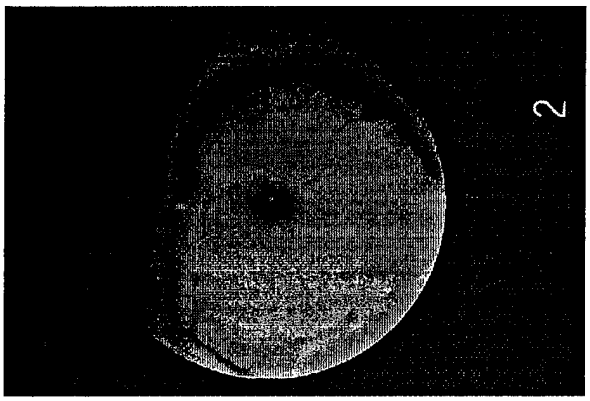

Fig. A5 & A6: CY 1507 (animal #3). This animal shows white dot lesions about 8 degrees inferior and superior-temporally at about 5 degrees. The temporal site is clear, and the foveal site may have an MVL.

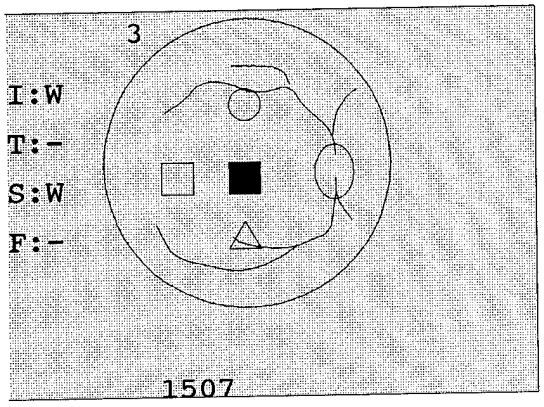

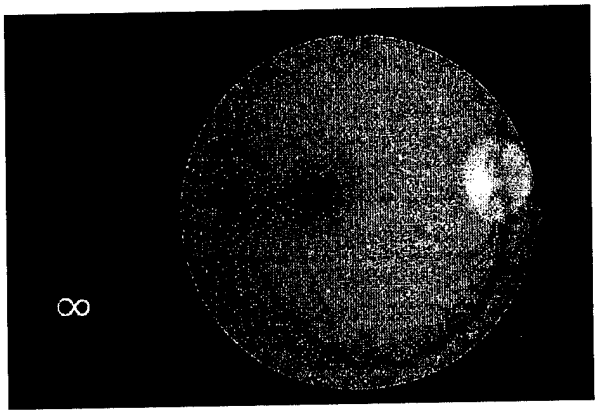

Fig. A7 & A8: CY 1159 OD (animal #4) This animal shows a bridging scar between the superior and the foveal sites (a red dot and a white dot lesion, respectively). The temporal site also shows a white dot lesion, while the inferior site is clear.

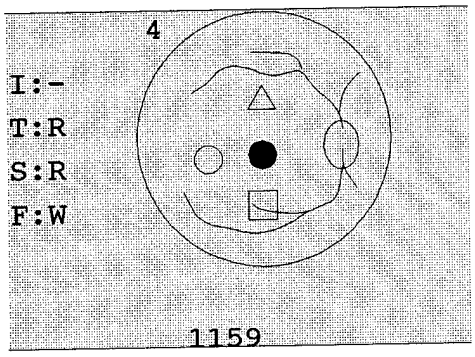

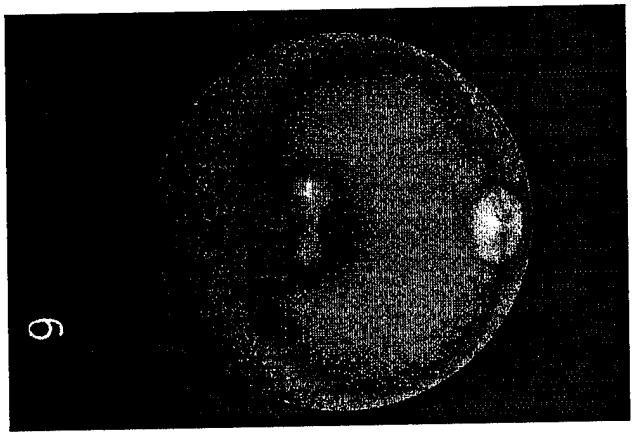

Fig. A9 & A10: CY 1137 OD (animal #5: deceased). This animal has its lesions photographed from the fixed eye cup rather than in vivo. The fovea was targeted for a white dot and the temporal site for a red dot exposure; both are still visible, although the foveal site was noted only as MVL at exposure. The inferior site was also noted with an MVL.

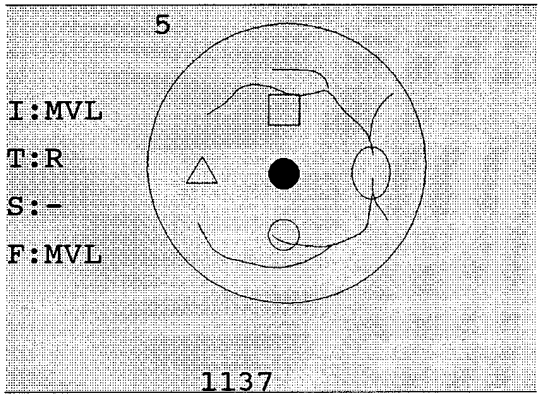

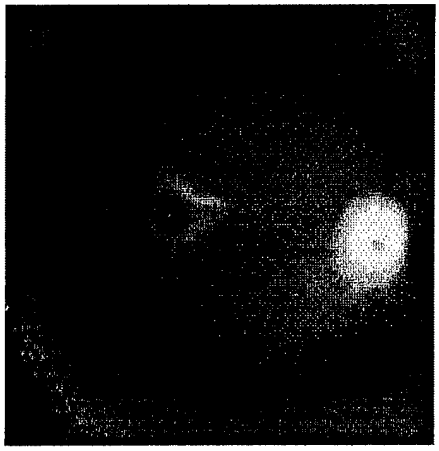

Fig A11 & A12: CY 10757 (animal #6: deceased). This animal was photographed through early cataracts. There are 3 lesions visible, at the inferior, foveal and superior sites, all apparently white dot, although the superior lesion is brighter than the others. The temporal site seems clear.

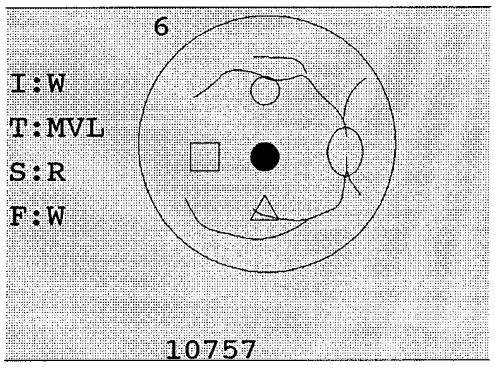

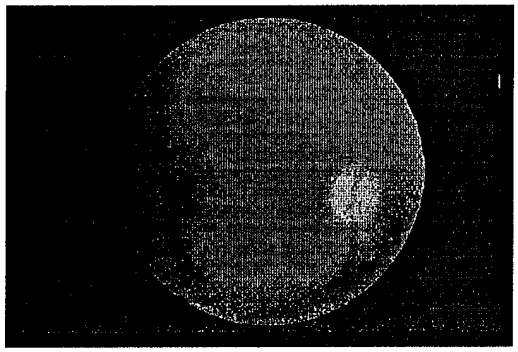

Fig. A13 & A14: CY 1209 OD (animal #7). This animal appears to have a circumscribed lesion (white dot) superior to the fovea. The fovea has a lesser lesion, even though it was classified as a red dot lesion at the time of exposure. The temporal site may have a lesion as well.

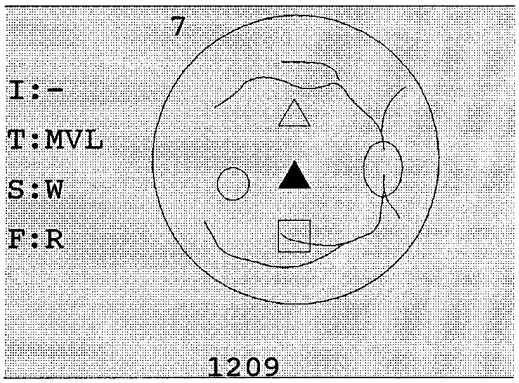

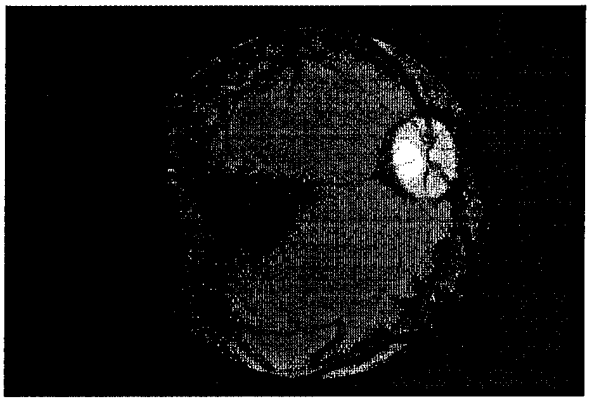

Fig A15 & A16: CY 12029 OD (animal #8). This animal has a red dot lesion in the fovea, and was noted at the time of exposure to have a white dot lesion temporally. Despite the poor quality of this image, both lesions remain large and obvious,

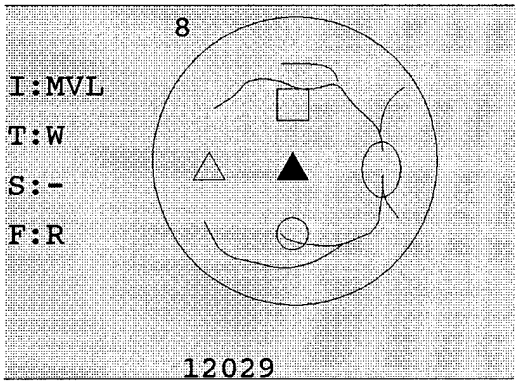

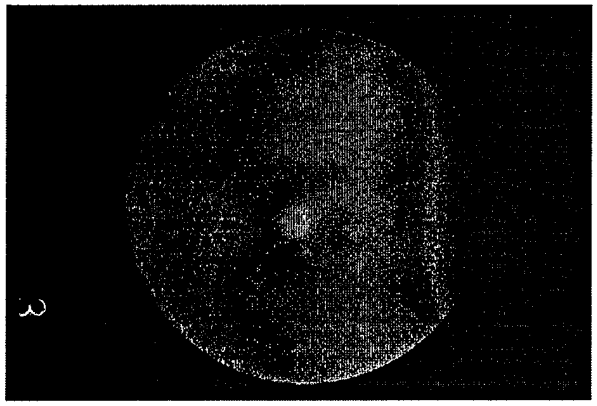

Fig. A 17 & A 18: CY 12043 OD (animal #9). This animal has a foveal red dot lesion, and was noted to have an inferior white dot lesion. The inferior lesion remains more obvious than the still visible foveal lesion. The superior site was scheduled for a white dot lesion; however no obvious changes can be noted at the site.

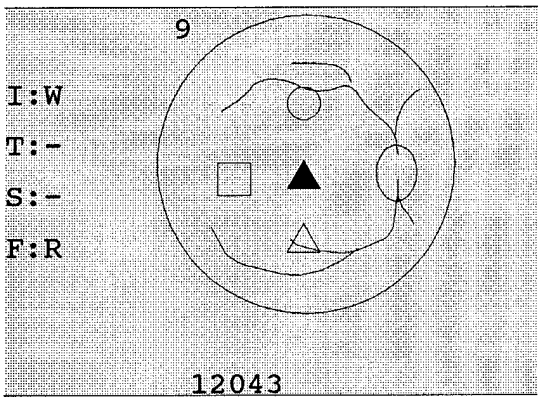

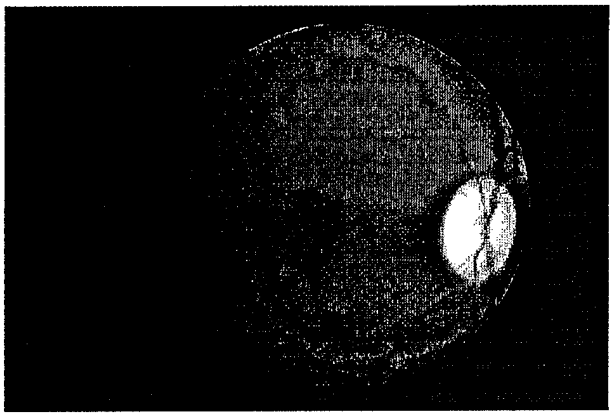

Midterm Report:

Figures (2)

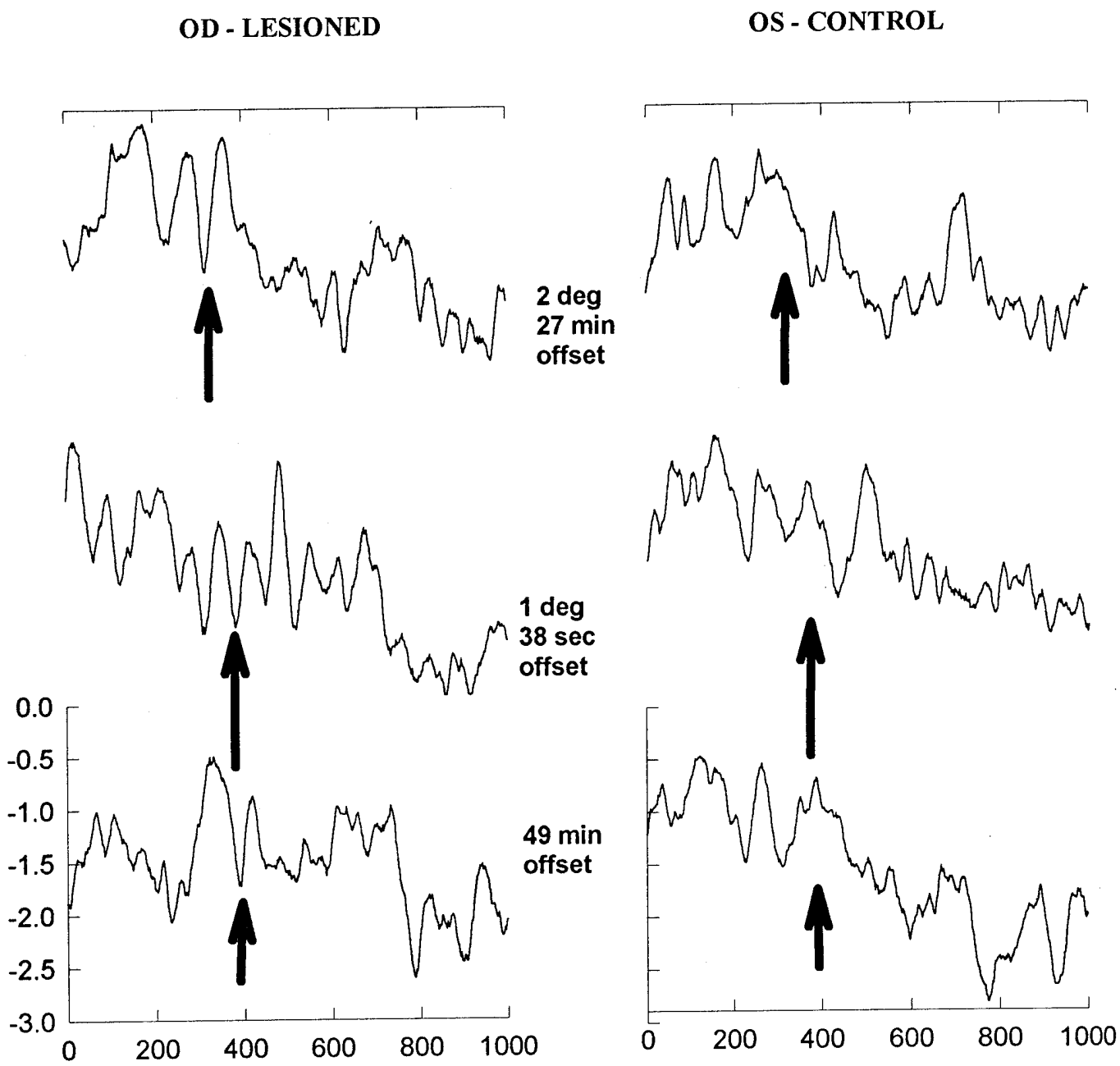

Fig. 1: Monkey vernier VEP recorded from posterio-lateral scalp referenced to eyebrow, Cz common. Arrows point out apparent responses OS & equivalent times OD.
Records from CY 1159 (OD: foveal white dot, bridging scar to superior red dot lesion, temproal red dot lesion). VEP acuity severely degraded OD.

Fig. 2: Human Vernier VEP
The VEP was recorded from Oz referenced to Fpz, A1 common. The main response is a P-N-P complex as noted, that scales with vernier offset.